AJIT KUMAR PANDEY
AMIT KUMAR
AJIT KUMAR
and
NITISH KUMAR

Steady-state and sensitivity analysis of a closed-circuit hydrostatic transmission used in side discharge loader, a typical mining equipment

Hydraulic drive systems play a vital and significant role in the mining and construction equipment. It gives a smooth change in the output speed, torque, and power of the machine.. Regulation of the displacements of the pump and the hydro-motor of the drive facilitates the control of the straight running and steering of the machines. The present study deals with the performance analysis of hydrostatic drive similar to that is incorporated in an SDL machine. It consists of a variable displacement pump rotated by a constant speed electric motor and a variable displacement hydro-motor. They are connected in the closed-circuit configuration. The present study investigates the performances of the hydrostatic drive used in the SDL machine through detailed modelling and experimentations. The study finds a reasonable efficiency zone for the design guideline to operate the hydrostatic drive. The effect of perturbation of critical system parameters on the dynamic performance of the drive has been also studied through simulation of the developed model. The outcome of the present work should be expedient for the preliminary design and assortment of similar hydraulic drive used in the mobile, mining equipment.

Keywords: *Closed-circuit hydrostatic drive, pump, hydro-motor, displacement ratio, overall efficiency*

1. Introduction

Heavy earthmoving machines such construction (erection) vehicles, cultivation, and forestry machines are usually propelled by hydrostatic drive due to its superior power density, widespread speed range and have good overall efficiency. This gives a clear advantage for such type of drive over electrical or mechanical solutions. In mobile vehicle, generally closed loop topology of the hydrostatic drive is used [1]. A hydrostatic transmission is a continuously variable transmission (CVT) that smoothens power transmission without the use of gear. Even though they are not extremely efficient compared to electric CVTs, the hydrostatic components are economical and have better energy storage capacity as compared to electrical components. Most of the vehicles require high tractive forces when starting and climbing. It may require 10-30 times more tractive force as compared to normal execution with standard load. Vehicle speed and load changes over a full range need maximum tractive effort when starting under full load. Energy efficiency and reduction of harmful emissions are the main challenges for the research concerning on and off the road vehicles. In this respect a systematic approach to control the hydraulic drives has been presented by Murrenhoff [2]. Helduser [3] investigated the performance of electric-hydrostatic drive systems and its components. It was shown that the efficiency of hydraulic components was better than that of variable speed electric motor. For wide range of operation, hydrostatic transmission with variable displacement setting of piston pump with fixed displacement motor has better efficiency than variable speed driven fixed displacement piston pump with fixed displacement motor. Mandal et al. [4, 5] have presented steady-state model of a closed circuit hydrostatic transmission. Such studies identify piston pump and the bent axis hydro-motor critical parameter and their effect on the performance of the system. Recently, Niranjan et al. [6] have studied the steady-state performance of high speed low torque (HSLT) hydrostatic summation drive using bent-axis motor. Such studies identify the operating range of the drives for a mining vehicle using single and double bent axis hydro-motors with reasonable accuracy. By controlling the piston pump displacement and shifting the drive mode from single motor to twin motor or vice-versa, such drive system may be useful for the machine having the wider torque-speed demand. Wang et al [7]. have experimentally investigated the performance of an open-circuit variable-speed-driven pump controlled motor drive system. They have shown that the performance of the said

Blind peer reviews carried out

Messrs. Ajit Kumar Pandey, Amit Kumar, Nitish Kumar, Department of Mechanical Engineering, National Institute of Technology, Patna, Bihar 800005 and Ajit Kumar, Department of Mining Machinery Engineering, IIT(ISM), Dhanbad, Jharkhand, 826004. E-mail: ajit.saurabh100@gmail.com / amit@nitp.ac.in; ajit.ism185@gmail.com / anupam.me@nitp.ac.in / nitish.me15@nitp.ac.in

drive at low torque and speed is found to be better than other variable displacement pump controlled motor system. Pfeiffer et.al [8] has proposed a numerical model for the hydrostatic transmission to improve the engine efficiency. In this study, detailed modelling of such transmission has not been done, only the efficiency characteristics of the engine have been considered. The conclusion form their work is drawn assuming 100% efficiency of the transmission. Pettersson and Tikkenen [9] have proposed both open and closed circuit secondary controlled swing drive of a hydraulic excavator and it has been concluded that they can save more as compared to the hybrid drive. Rahmfeld and Skirde [10] analyzed the efficiencies of the bent axis hydro-motor and swash plate controlled piston pump at their different angle.It has been concluded that their precise loss models can accurately predict their performance. However, combining them, the performance of the system has not been analyzed. More recently Manring [11] has proposed a model of closed circuit primary controlled transmission to generate efficiency map for first approximation to assess the transmission efficiency. However, the detail experimental results are not presented to validate the model. To control the variable displacement pump and variable displacement motor, a control algorithm (HABB) was introduced by Wang et al. [12]. Simulation outcomes of the said control algorithm suggested shows a very good response as well as robustness over the change in the drive operating parameters. The thermal effect on the slipper bearing of axial piston pump was investigated by Tang et al. [13]. The results shows that to improve the capacity of slipper bearing, condition of higher thermal conductivity is favourable but not at cost of thermal equilibrium clearance.

The influence of thermal effect on hydrostatic slipper bearing capacity of axial piston pump was investigated. Conventionally, in various hydrostatic drives, a standard control approach is employed to determine the driveline settings (the volumetric displacement of motor and volumetric displacement, speed of the piston pump) when a particular speed of the vehicle is needed. In this approach, if energy efficiency is not an objective, two different stages may be practiced to control the speed of the bent axis hydro-motor. For a constant speed driven piston pump in primary controlled mode of operation, when speed of the vehicle is low, the displacement setting of the bent axis hydro-motor is set at the maximum limit. By doing so the motor has the maximal torque to pressure ratio. Therefore, the bent axis hydro-motor can deliver its maximum torque and accelerate the load, if needed. If the speed is required to be increased the displacement of the piston pump is also increased. When the swash plate angle of the piston pump attains its maximum limit, the second stage starts. At this stage that is in secondary controlled mode of operation of the drive, an increase of the vehicle speed is achieved by reducing the displacement setting of the bent axis hydro-motor. A schematic representation of the piston pump and the motor displacement control is shown in Fig.1.

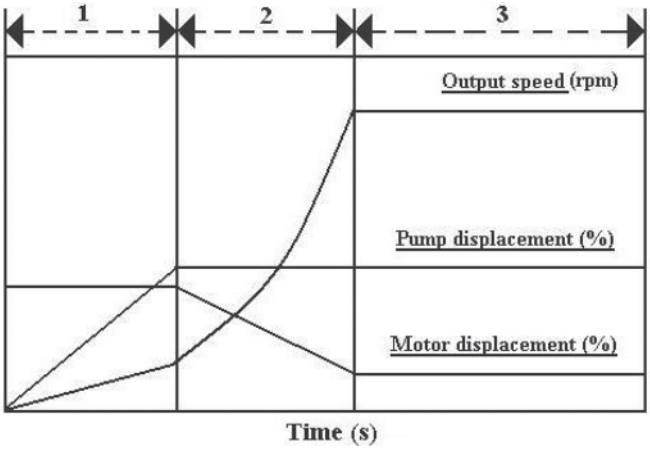

Fig.1: Standard speed control

Therefore, by choosing the control parameter settings, it can be possible to run the transmission at optimum energy settings.

2. Physical system

Fig.2 illustrates a simplified diagram of the closed circuit hydrostatic transmission considered for the studies. An electric motor which acts as a prime mover turns a variable displacement piston pump at a constant speed which supplies pressurized hydraulic fluid to the bent axis hydro-motor that in turn drives the load. The piston pump and the bent axis hydro-motor are changeable in volumetric displacement controlled through electrical or hydraulic signal. A positive suction head is provided to the piston pump. The

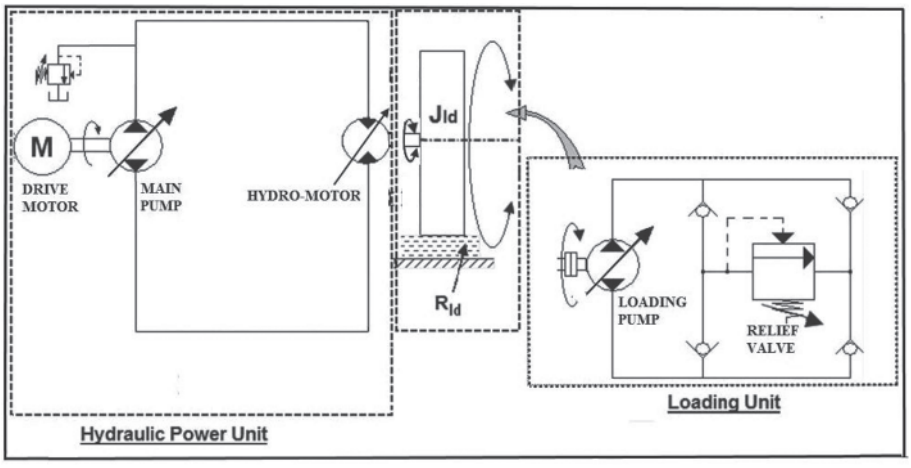

Fig.2: Closed ciruict hydrstatic drive

bent axis hydro-motor drives a loading piston pump. By regulating the displacement setting of the piston pump or by adjusting pressure of the relief valve, load on the bent axis hydro-motor is varied. A compact form of closed circuit hydrostatic transmission considered for the analysis is presented here, however, in actual practice with the presented schematic circuit, it includes a charge piston pump to feed the loop for leakage losses, cross-over relief valve for safety, flushing unit to maintain the temperature. For a more detailed diagram, the interested reader is referred to standard text books [14].

A bent axis hydro-motor is a rotary actuator that converts hydraulic power into mechanical power. It works in combination with a hydraulic piston pump that converts mechanical power of the electric motor into hydraulic power of the hydraulic fluid. A variable displacement bent axis hydro-motor can drive a load at a different speed for a fixed input flow. A bent-axis variable displacement hydro-motor considered for the analysis [15] is shown in Fig.3, which has seven pistons in numbers that reciprocate within a cylinder block. The pistons are put in a circular order inside a housing of a cylinder block with an angle to the main drive shaft and separated with equal angular space. The angle between the axis of the cylinder block and the drive shaft known as swivel angle is adjusted by the control unit, where a control piston turns the cylinder block through control lens. By doing so, the speed and the torque of the bent axis hydro-motor are varied.

The hydrostatic machine has different gaps for the design requirement, particularly between the parts having relative motion to each other. The fluid flows through the gap due to a pressure difference. Various leakage flow paths of the piston pump [16] and the bent axis hydro-motor considered for the analysis are shown in Figs.3 and 4. They are as follows:

(a) Gap within the piston and the barrel hole (Q_{al}).

(b) Gap within the ball and socket joint (Q_s).

(c) Gap within the valve plate and cylindrical barrel (Q_d).

Combining the above leakages, they are considered as external leakage flow resistance of the piston pump and the bent axis hydro-motor.

(d) Cross-port flow loss (Q_{ilm}) where fluid flow back from inlet to outlet port (in case of motor) known as internal leakage

(e) Cross-port flow loss (Q_{ilp}) where fluid flow back from the outlet to inlet port in case of piston pump) known as internal leakage.

3. Experimental set-up and its working

In order to provide a basis for the hydraulic components experimental identification and model validation, the closed-circuit drive has been built up. Fig.5 shows a schematic illustration of the same. The test set-up incorporates the commercially available pump, motor and the proportional pressure relief valve (PPRV). While Fig.5 shows schematic of the experimental test rig along with the instrumentation, Fig.6 shows its pictorial view.

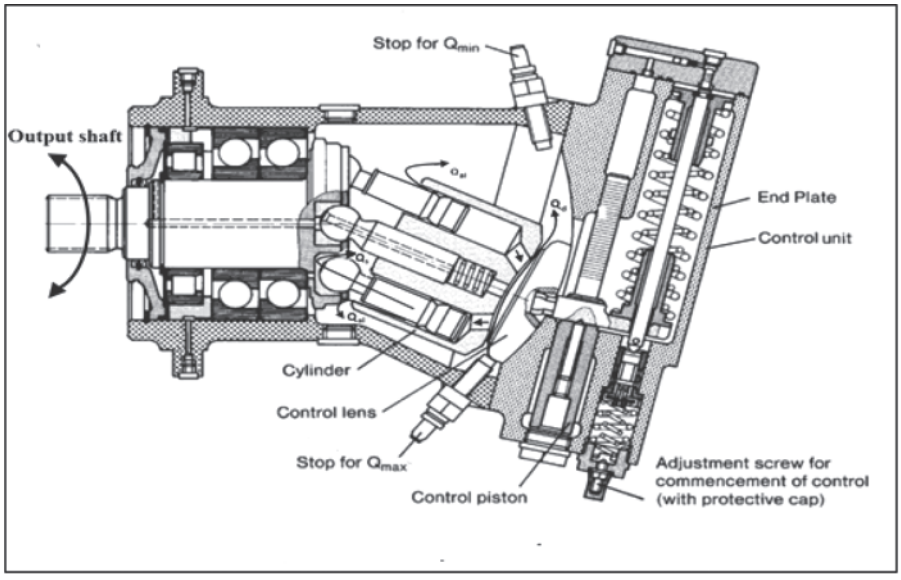

Fig.3: Variable displacement bent axis hydro-motor [15]

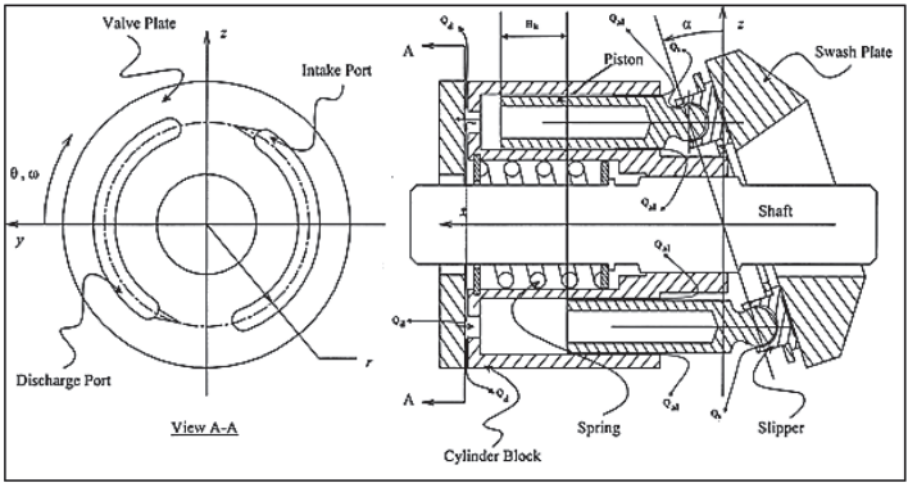

Fig.4: Variable displacement axial piston (swash plate design) pump [16]

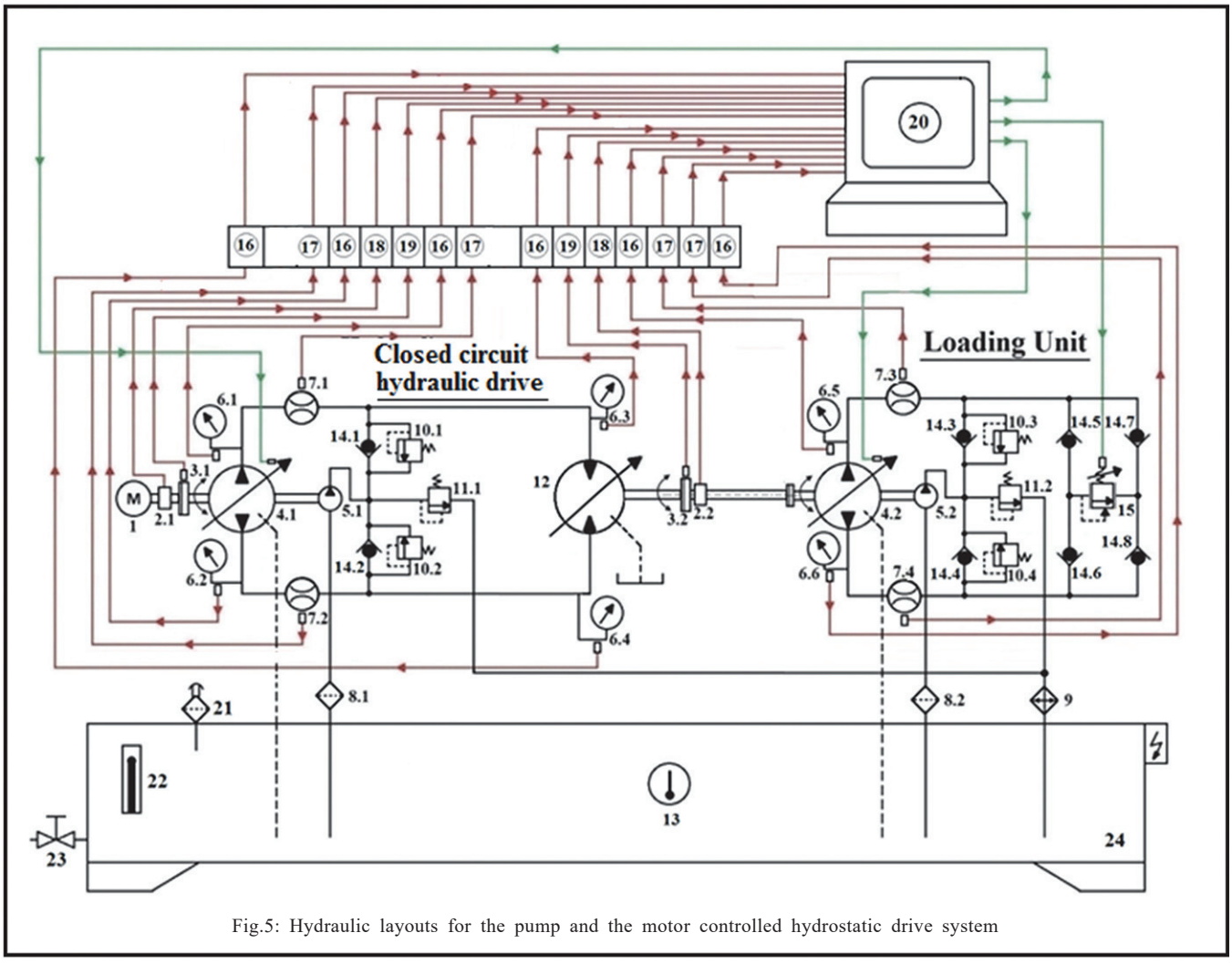

Fig.5: Hydraulic layouts for the pump and the motor controlled hydrostatic drive system

An induction motor (1) rotating nearly at a constant speed drives a variable displacement pump (2) that supplies pressurized fluid to a variable displacement hydro-motor (3). The hydro-motor rotates the load directly. The maximum test pressure was limited to 250 bars. The charge pump of the test set-up maintained 20 bar at the low-pressure P_{mo} side of the drive. The load on the hydro-motor is provided by a loading circuit. The oil cooler maintained the oil temperature at 50 ± 2ºC to keep the fluid viscosity constant with fair accuracy.

4. Model of the closed-circuit pump-motor system

Fig.7 shows the model of the closed-circuit HST. The SF element indicates pump speed N_p. The activated I element on 0_{Tp} junction records the pump torque, whereas element R on 1_{Np} junction denotes the pump drag resistance (R_{fp}). In the model, $0p_{po}$, $0p_{pi}$ junctions indicate the plenum of the outlet and the inlet ports of the variable pump, respectively; similarly $0p_{mi}$, $0p_{mo}$ junctions represent the same for the variable displacement motor. The C elements attached with them denote the equivalent fluid bulk stiffness (K_p and K_m)

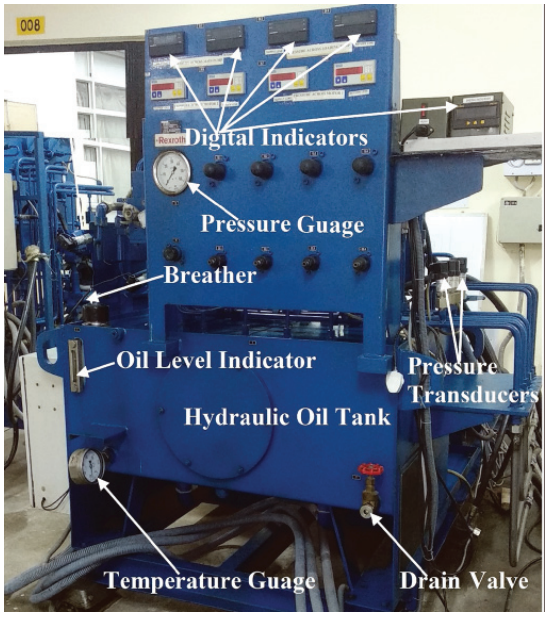

Fig.6: Experimental test set-up of the hydrostatic drive system

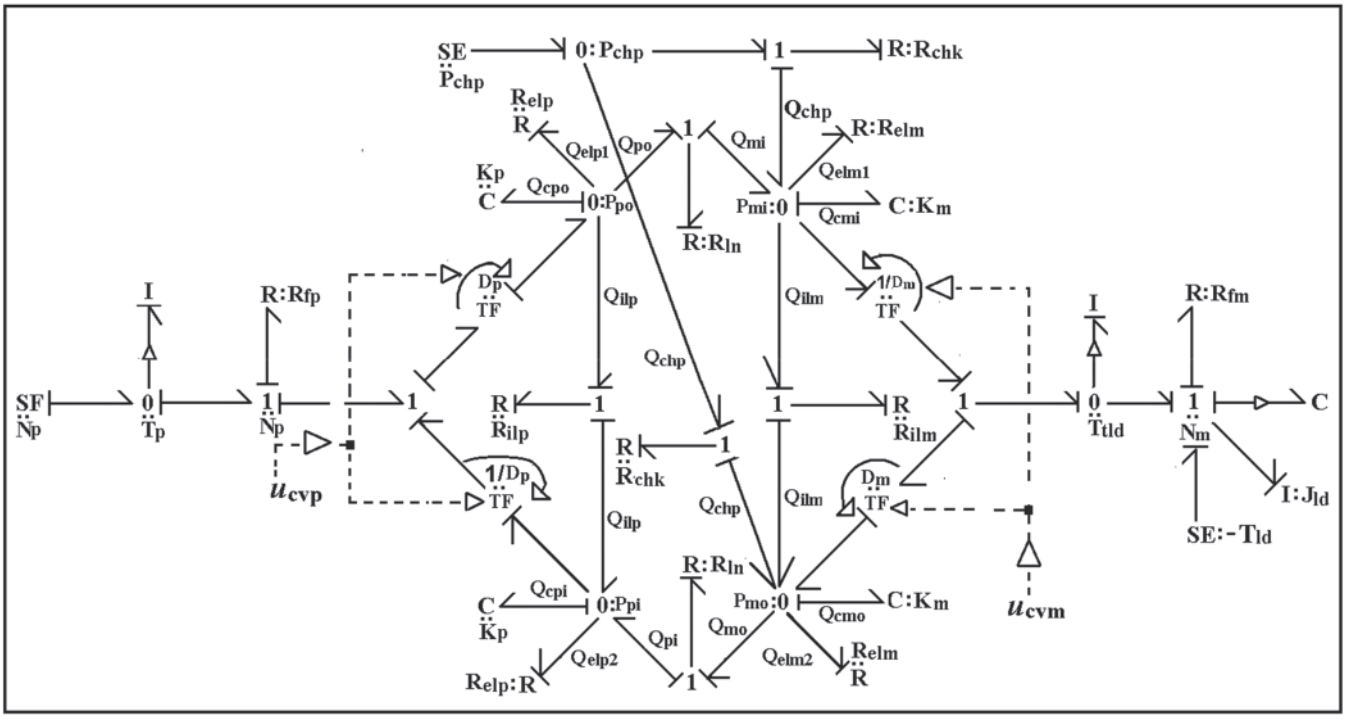

Fig.7: Model of the closed-circuit hydraulic drive

that take into account the compressibility flow losses; whereas, the resistive elements (R) attached with the 0 junction represent leakage coefficients (R_{elp}, R_{elm}, R_{ilm}, R_{ilp}) of the hydraulic pump and the motor. In a hydraulic drive, a pump changes mechanical energy into hydraulic energy; whereas, in the case of a hydro-motor it is vice-versa. Such a transformation of power is depicted in the model by a TF element. The moduli of the TF elements are the displacement rate of the pump and the motor (Q_p=D_p×N_p). The modulation of D_p and D_m by the respective command signals u_{cvp} and u_{cvm} is indicated by the arrows of the dotted lines connected with the MTF junctions. From the pump plenum indicated by the 0ppi junction, the flow Q_{mi} is supplied to the motor inlet port 0pmi junction overcoming the line resistance R_{ln}. Similarly, the outlet flow from the motor Q_{mo} returns to the pump inlet port at $0p_{pi}$ junction.

The SE element connected with the $0p_{chp}$ junction indicates the flow from a fixed pressure source provided by the boost pump. Through the check valve, the said flow is supplied to the low-pressure line that connects the main pump and the hydro-motor. The R element on the $1Q_{chp}$ junction takes into account the check valve resistance (R_{chk}). In the event of the low pressure created at either side of the supply or the return line of the hydro-motor, it allows flow Q_{chp} from pressure P_{chp} to either of the lines through the respective check valve. The check valve resistance R_{chk} is low when the charge pressure P_{chp} is more than the line pressure (P_{mi} or P_{mo}). It is vice-versa; when P_{mi} or P_{mo} is more than P_{chp}. The activated I element with 0_{Tld} junction monitors the load torque (T_{tld}) of the hydraulic motor. The I and R elements attached with the 1Nm junction represent the load inertia J_{ld} and motor viscous friction R_{fm}, respectively; whereas, the SE elements indicates the load torque (T_{ld}) and the activated C element records the drive speed N_m.

4.1 Equations of the test system

Referring to Fig.7, the compressibility flow losses of the fluid at the outlet and the inlet plenum of the variable displacement pump are

$$Q_{cop} = D_p N_p - Q_{elp1} - Q_{ilp} - Q_{po} \quad \text{... (1)}$$

$$Q_{cpi} = -D_p N_p + Q_{ilp} - Q_{elp2} - Q_{pi} \quad \text{... (2)}$$

In Eqn.1, the third and fourth terms signify the leakage flow from the pump outlet port and the internal leakage of the pump, respectively; whereas, the fifth term represents the pump outlet flow. Similarly, in Eqn.2, the fourth and fifth terms indicate the leakage flow from pump inlet port and the pump inlet flow, respectively.

The compressibility flow losses of the fluid at the inlet and the outlet ports of the hydro-motor are

$$Q_{cmi} = Q_{mi} + Q_{chp} - Q_{elm1} - Q_{ilm} - D_m N_m \quad \text{... (3)}$$

$$Q_{cmo} = D_m N_m + Q_{ilm} + Q_{chp} - Q_{elm2} - Q_{mo} \quad \text{... (4)}$$

In Eqn.3, the second and third terms indicate the motor inlet flow and charge pump flow. The fourth and fifth terms represent the leakage flow from the motor inlet port and the internal leakage of the motor, respectively. Similarly, in Eqn.4, the fifth and the sixth terms indicate the leakage flow from motor outlet port and the motor outlet flow, respectively.

The pump input torque

$$T_p = D_p (P_{po} - P_{pi}) + N_p R_{fp} \quad \text{... (5)}$$

The pump pressure at its supply and return ports are given by

$$P_{po} = K_p \int Q_{cpo}\, dt \quad \text{... (6)}$$

$$P_{pi} = K_p \int Q_{cpi}\, dt \quad \text{... (7)}$$

The pressure at the inlet and outlet ports of the hydro-motor are given by

$$P_{mi} = K_m \int Q_{cmi}\, dt \quad \text{... (8)}$$

$$P_{po} = K_m \int Q_{cmo}\, dt \quad \text{... (9)}$$

Considering the torque balance at 1 junction, the inertia torque of the motor shaft is

$$T_{ild} = D_m (P_{mi} - P_{mo}) - R_{fm} N_m - T_{ld} \quad \text{... (10)}$$

In Eqn. 10, the second, third and fourth terms represent that motor torque, torque loss due to viscous friction of motor and the load torque on the motor shaft, respectively.

Rearranging Eqn. 10, at steady-state, the torque load T_{ld} is

$$T_{ld} = D_m (P_{mi} - P_{mo}) - R_{fm} N_m \quad \text{... (11)}$$

The hydro-motor speed

$$N_m = \int \frac{T_{ild}}{J_{ld}} dt \quad \text{... (12)}$$

In the above equation, J_{ld} is the inertia load on the hydro-motor shaft.

4.2 Steady-state equations of the model

In the closed-circuit hydrostatic drive considered for the analysis, the pump and the motor are closed to each other. Therefore, the supply and the inlet pressures of the pump are equal to the inlet and return pressures of the hydro-motor. Considering the said fact, in Eqns. (1) through (4),

$P_{po} = P_{mi} = P_1$, $P_{pi} = P_{mo} = P_2$,

$Q_{po} = Q_{mi} = Q_1$, and $P_{mo} = Q_{pi} = Q_2$,

The leakage flow of the pump and the hydro-motor may be expressed as

$$Q_{elp1} = \frac{P_{mi}}{R_{elp}} = \frac{P_1}{R_{elp}}$$

$$Q_{elp} = \frac{(P_{mi} - P_{mo})}{R_{ilp}} = \frac{(P_1 - P_2)}{R_{ilp}}$$

$$Q_{elp2} = \frac{P_{pi}}{R_{elp}} = \frac{P_2}{R_{elp}}$$

$$Q_{elp1} = \frac{P_{mi}}{R_{elm}} = \frac{P_1}{R_{elm}}$$

$$Q_{ilp1} = \frac{(P_{mi} - P_{mo})}{R_{ilm}} = \frac{(P_1 - P_2)}{R_{ilm}}$$

$$Q_{ilp2} = \frac{P_{mo}}{R_{elm}} = \frac{P_2}{R_{elm}}$$

Ignoring the flow loss due to fluid compressibility, the steady-state equations of the model are obtained. Following equations express the steady-state outlet and the inlet flow of the pump obtained from Eqns. (1) and (2).

$$Q_1 = D_p N_p - \frac{P_1}{R_p} + \frac{P_2}{R_{ilp}} \quad \text{... (13)}$$

$$Q_2 = D_p N_p - \frac{P_1}{R_{ilp}} + \frac{P_2}{R_p} \quad \text{... (14)}$$

In Eqns. (13) and (14)

$$\frac{1}{R_p} = \frac{1}{R_{elp}} + \frac{1}{R_{ilp}}$$

The charge pump maintains a constant pressure in the return line of the closed-circuit drive. Ignoring the charge pump flow (Q_{chp}) in the return line at steady-state, which is usually the practice, the following equations express the inlet and the outlet flows of the motor obtained from Eqns. (3) and (4).

$$Q_1 = D_m N_m + \frac{P_1}{R_m} - \frac{P_2}{R_{ilm}} \quad \text{... (15)}$$

$$Q_2 = D_m N_m + \frac{P_1}{R_{ilm}} - \frac{P_2}{R_m} \quad \text{... (16)}$$

In Eqns. (15) and (16)

$$\frac{1}{R_m} = \frac{1}{R_{elm}} + \frac{1}{R_{ilm}}$$

Equating Eqns. (13) and (15)

$$\frac{N_m}{N_p} = \frac{D_p}{D_m} - \frac{P_1}{D_m N_p}\left(\frac{1}{R_p} + \frac{1}{R_m}\right) + \frac{P_2}{D_m N_p}\left(\frac{1}{R_{ilp}} + \frac{1}{R_{ilm}}\right) \quad \text{... (17)}$$

From Eqn. (11)

$$\frac{N_m}{N_p} = \frac{D_p}{R_{fm}}\left(\frac{P_1 - P_1}{N_p}\right) - \frac{T_{1d}}{N_p R_{fm}} \quad \text{... (18)}$$

Equating Eqns. (3.17) and (3.18)

$$P_1 = \frac{C_1}{A_1} \quad \text{... (19)}$$

where,

$$A1 = \left(\frac{1}{D_m N_p}\right) R1 + \frac{D_m}{R_{fm} N_p}; \text{ where } \frac{1}{R_1} = \frac{1}{R_p} + \frac{1}{R_m}$$

$$B1 = \frac{D_m}{R_{fm}} + \frac{1}{D_m R_2} \text{ ; where } \frac{1}{R_2} = \frac{1}{R_{ilp}} + \frac{1}{R_{ilm}}$$

$$C1 = \frac{D_p}{D_m} + \frac{P_2 B1}{N_p} + \frac{T_{ld}}{N_p R_{fm}}$$

Substituting P_1 from Eqn. (19) into Eqn. (18), the predicted speed of the hydro-motor

$$N_{mp} = N_p D1 \quad \text{... (20)}$$

where, $$D1 = \frac{D_p}{D_{fm}}\left(\frac{\frac{C1}{A1} - P2}{N_p}\right) - \frac{T_{ld}}{N_p R_{fm}}$$

Substituting P_1 from Eqn. (19) in Eqn. (5), the predicted pump torque

$$T_{pp} = D_p\left(\frac{C1}{A1} - P2\right) + N_p R_{fm} \quad \text{... (21)}$$

From Eqn. (19), the predicted load torque

$$T_{1dp} = (P_1 - P_2) D_m - R_{fm} N_{mp} \quad \text{... (22)}$$

$$T_{1dp}\left(\frac{C1}{A1} - P2\right) D_m - R_{fm} N_{mp}$$

Subtracting Eqn. (14) from Eqn. (13)

$$R_{elp} = \frac{P_1 + P_2}{Q_2 - Q_1} \quad \text{... (23)}$$

From Eqn. (13)

$$R_{ilp} = \frac{(P_1 - P_2)}{(D_p - N_{elp} - Q_1)} \quad \text{... (24)}$$

Subtracting Eqn. (15) from Eqn. (16)

$$R_{elm} = \frac{P_1 + P_2}{Q_1 - Q_2} \quad \text{... (25)}$$

Adding Eqns. (15) and (16)

$$R_{ilm} = \frac{(P_1 - P_2)}{(Q_1 - Q_2)} - D_m N_{ma} - \frac{(P_1 - P_2)}{2R_{elm}} \quad \text{... (26)}$$

From Eqn. (5)

$$R_{fp} = T_{pa} - D_p \frac{(P_1 - P_2)}{N_p} \quad \text{... (27)}$$

From Eqn. (11)

$$R_{fm} = \frac{(P_1 - P_2) D_m - T_{ld}}{N_{ma}} \quad (28)$$

Substitution of the test data of T_{pa}, T_{ld}, Q_1, Q_2, N_{ma}, N_p, P_1, P_2, Q_{elp}, Q_{elm} for different values of T_{ld} in the Eqns. (23) through (28) characterize the loss coefficients (R_{elp}, R_{ilp}, R_{elm}, R_{ilm}, R_{fp}, R_{fm}). Their characteristics are obtained at both pump and the hydro-motor controlled mode of operations (varying displacements of the pump and the hydro-motor) of the closed-circuit hydrostatic drive.

The following equations express the predicted performance parameters of the drive.

The torque loss

$$T_{1sp} = N_p R_{fp} + N_{mp} R_{fm} \quad \text{... (29)}$$

The load torque

$$T_{1dp} = (P_1 - P_2) D_m - R_{fm} N_{mp} \quad \text{... (30)}$$

The output power

$$W_{pd} = N_{mp} T_{ldp} \quad \text{... (31)}$$

The slip of the drive

$$S_p = \frac{(N_{mi} - N_{mp})}{N_{mi}} \quad \text{... (32)}$$

The overall efficiency of the drive

$$\eta_{op} = \frac{T_{ldp} N_{mp}}{T_{pp} N_p} \quad \text{... (33)}$$

The following equations give the actual performance parameters of the drive.

$$T_{1sa} = T_{pa} - (P_1 - P_2)(D_p + D_m) - T_{ld} \quad \text{... (34)}$$

$$W_{ad} = N_{ma} T_{ld} \quad \text{... (35)}$$

$$s_a = \frac{(N_{mi} - N_{ma})}{N_{mi}} \quad \text{... (36)}$$

$$\eta_{oa} = \frac{T_{ld} N_{ma}}{T_{pa} N_p} \quad \text{... (37)}$$

Using the relationships given in Eqns. (29) through (33), the predicted performance parameters are obtained for different load torque (T_{ld}) at pump and motor controlled mode of operations of the drive (varying displacements of the hydraulic components). The actual performance parameters obtained by using the test data in Eqns. (34) through (37) are compared to their predicted values to validate the steady-state model.

5. Experimental results and discussion

5.1 Verification of the overall leakage in pump and motor controlof the HST drive

The loss coefficients of the piston pump and the bent axis hydro-motor with respect to their displacement rate were determined experimentally. Considering maximum displacement of the motor, with respect to the piston pump displacement, the losses of the piston pump and the bent axis hydro-motor were determined. Similarly, the various losses were determined with the variation of the motor displacement. The characteristics of the overall flow loss (pump control) are identified. During experiment the hydrostatic drives are

operated in primary and secondary controlled mode; where the speed and torque ranges were kept around 500-3000 RPM and 15-75 Nm, respectively. The test-data were recorded through suitable sensors.

It is observed that the leakage flow of the drive (pump control) reduces with the rise in the displacement setting of the piston pump; whereas, with the rise in the load torque for a fixed displacement of the piston pump or the bent axis hydro-motor, the volumetric efficiency of the piston pump and the bent axis hydro-motor falls (Fig.8).

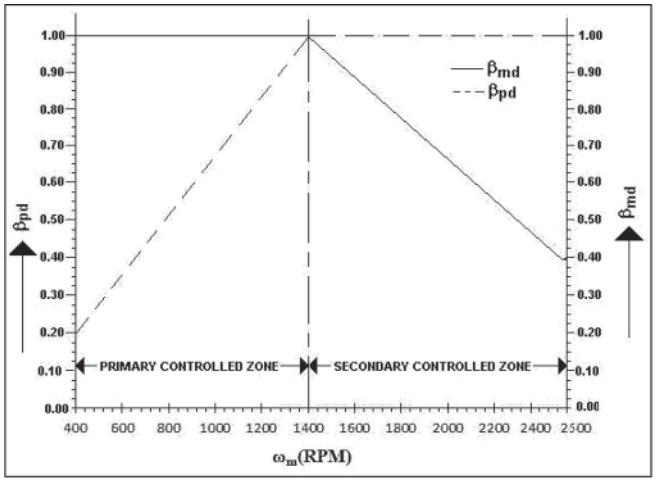

Fig.8: Variation of overall leakage (slip) of HST drive (pump control)

Similarly, it is observed that it is observed that the leakage flow of the drive in motor control increases with the lowering in the displacement setting of the hydro-motor; whereas, with the rise in the load torque for a fixed displacement of the piston pump or the bent axis hydro-motor, the volumetric efficiency of the piston pump and the bent axis hydro-motor falls (Fig.9).

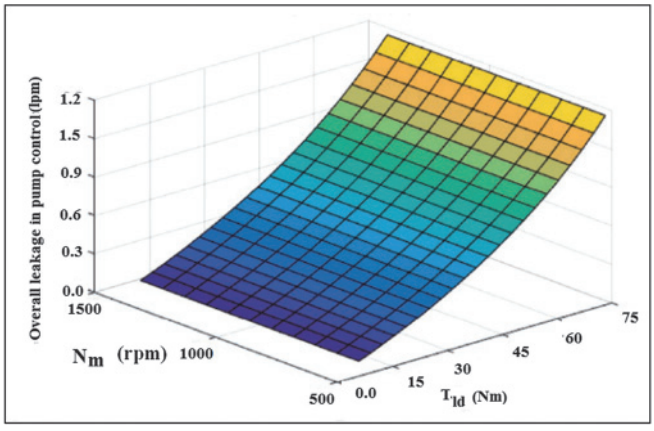

Fig.9. Variation of overall leakage (slip) of HST drive (motor control)

The valve port resistance of thebent axis hydro-motor that translates into its hydro-mechanical efficiency. Increase in the piston pump displacement decreases such resistance; whereas, increasing motor displacement its value increases. Increase in the torque level for a particular piston pump displacement, reduces port resistance; thereby hydro-efficiency of the motor improves, whereas, such efficiency falling off, with the rise inthe torque for a particular motor displacement (Fig.10).

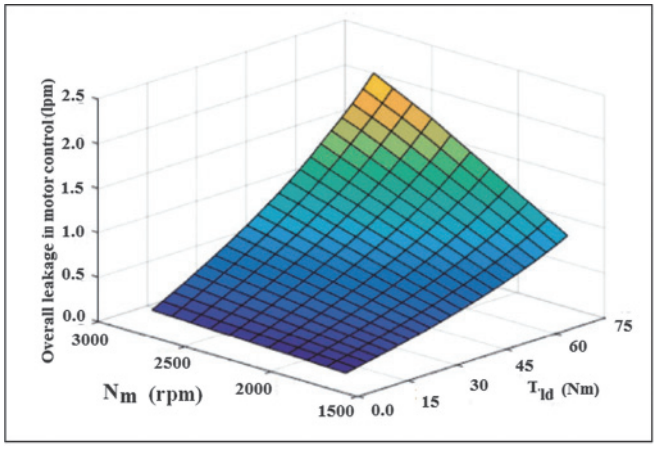

Fig.10: Variation of overall torque-loss (%) of HST drive (pump control)

Drag resistance decreases with the increase in the piston pump displacement, whereas, it increases with the increase in the bent axis hydro-motor displacement at the same torque level. The resistance R_{pd} rises with the rise in the torque level at a particular displacement of a piston pump or a bent axis hydro-motor. Like bent axis hydro-motor, such resistance contributes to the hydro-mechanical efficiency of the piston pump (Fig.11).

The variations of the above said losses were also recognized by McCandlish, D and Dorey [17] and Mandalet

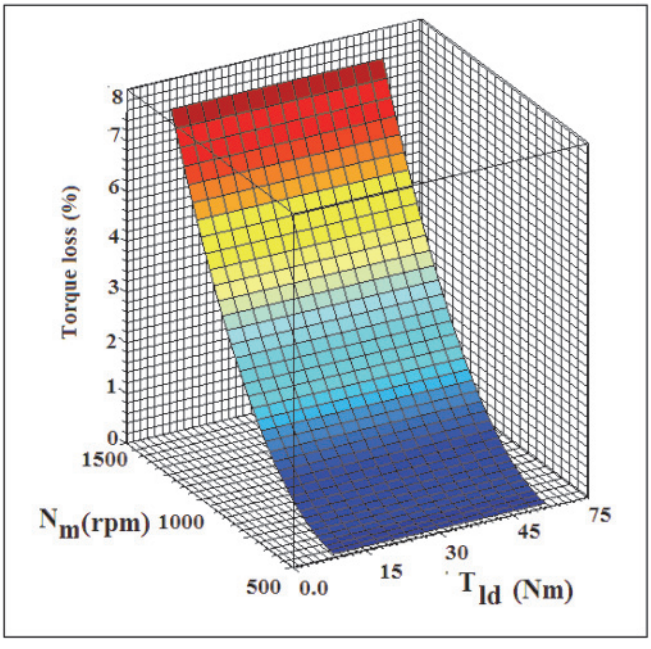

Fig.11: Variation of overall Torque-loss (%) of HST drive (motor control)

al. [5] in their studies on the piston pump. The variation of R_{vi}explainedby the quadratic relationship, which was also founded by Thoma [18] and Schösser [19].

6. Performance parameters of the hydrostatic drive

The performance parameters like flow loss, torque loss and the overall efficiency of the hydrostatic transmission are considered with respect to the variation of the piston pump and the bent axis hydro-motor displacement to cover complete range of speed and torque.

The characteristics of the drive have been studied with respect to the primary and the secondary controlled mode of operations. During such studies the displacement of the piston pump and the bent axis hydro-motor are adjusted as shown in Fig.12.

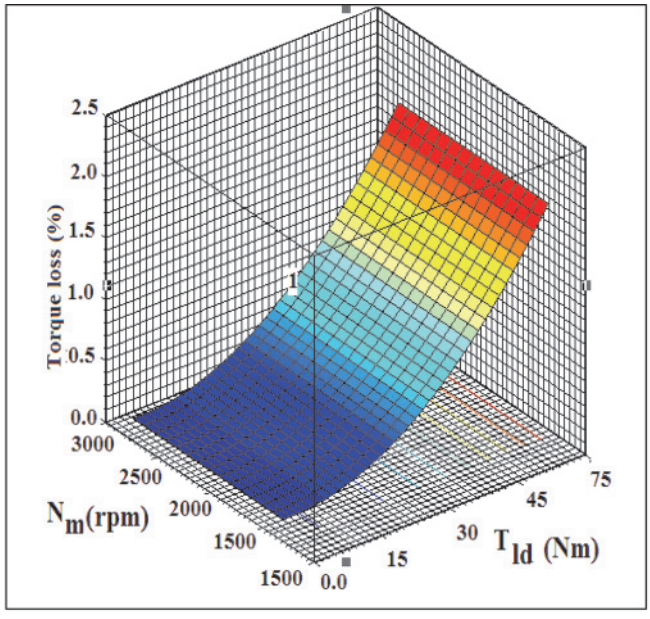

Fig.12: Variation of the displacement ratio of the piston pump (β_{pd}) and the bent axis hydro-motor (β_{md}) with speed

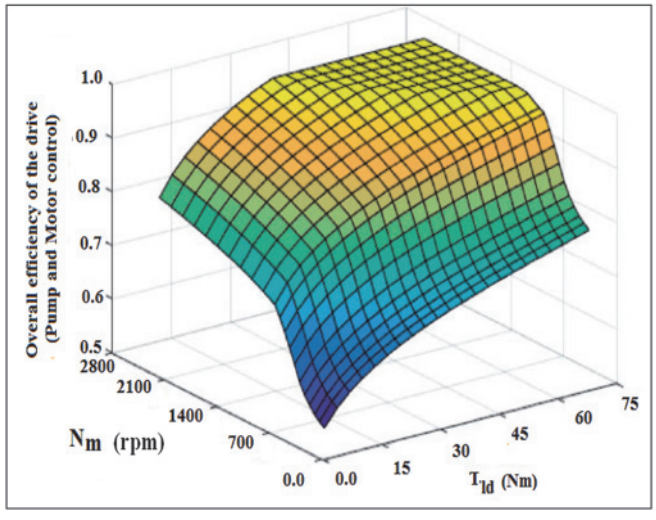

Fig.13: Overall driveefficiency

6.1 Slip the hydrostatic transmission

Slip of the hydrostatic drives is basically due to the leakage flow losses of the piston pump (R_{pl}) and the bent axis hydro-motor (R_{ml}). This contributes into the volumetric efficiency of the transmission as shown in Figs.8 and 9.

6.2 Torque loss of the hydrostatic drive

Major factors for the mechanicalloss of the hydrostatic transmission are the resistances offered by the valve port of the hydro-motor and drag resistance of the pump. This translates into the hydro-mechanical efficiency of the transmission as shown in Fig.10 and 11.

6.3 Overall efficiency of the hydrostatic transmission

The volumetric and the hydro-mechanical efficiencies both contribute to the overall efficiency of the hydro-static transmission.The efficiencies of the drive for the complete range of its operation is given in Fig.13

From the comparative study, the observations made are given below:

- The drive efficiency increases with the increase in speed up to 1400 rpm. During this speed range, the slip predominates over the torque losses of the drive as indicated in Fig.8.
- The efficiency of the hydrostatic drive decreases with increasing bent axis hydro-motor speed beyond 1400 rpm, where the torque losses predominate over the slip of the drive.
- The efficiency of the hydrostatic drives at a constant speed rises with rising torque level. This may be due to the fact that torque loss at a constant speed decreases at higher torque levels.

For the above observations, it may be concluded that the primary controlled drive is efficient in high torque and high speed operating condition; whereas the secondary controlled is found to have better efficiency in high torque and low speed operation.

This overestimation value may be attributed to the several other factors not considered while modelling as well as in the analysis, such as hydrodynamic losses, bearing friction, variation of leakages flow due to thermal effect, distortion over the mating contact surfaces and the quality of the mating surface finish, other additional leakage path etc.

7. Constant torque and constant power operations of the closed-circuit hydrostatic drive

In a hydraulic drive, when the pump speed and the pressure difference across the hydro-motor are maintained constant, the pump and the motor-controlled mode of operations are called constant torque and constant power traction drives, respectively. Equations (30) and (31) represent the predicted torque (T_{ldp}) and power ($W_{pd} = T_{ld} \times N_m$) of the hydrostatic drive system. Fig.14 (a) and (b) compare the ideal, predicted,

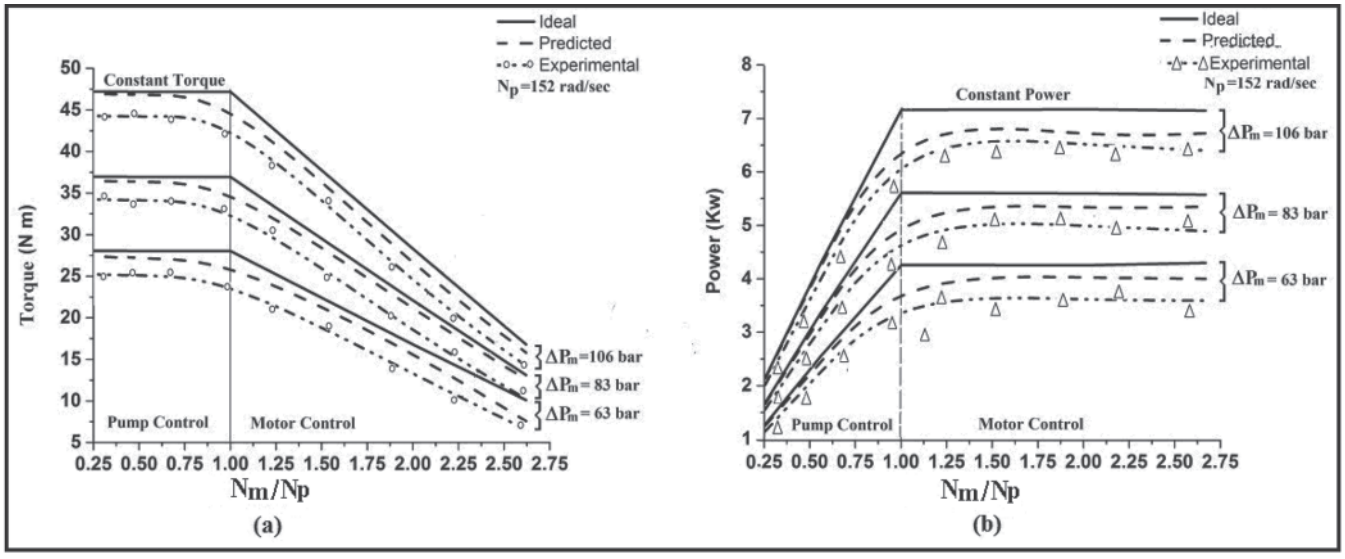

Fig.14: Traction drive performance of the closed-circuit hydrostatic drive system

and actual torque and power of the hydrostatic drive at different pressure levels across the hydro-motor. It may please be noted that the ideal drive's performance does not consider the said losses.

The variations of the torque and power of the drive with the speed ratio (N_m/N_p) are plotted at different "P_m values, considering the pump speed is 1500 rpm. It shows that the actual torque and power of the hydraulic motor of the system obtained from the steady-state measurement are lower than their predicted values. The differences between them may be due to the factors not accounted for while modelling discussed in the preceding section.

8. Sensitivity analysis

The wear and tear of the hydraulic components, drive system layout, frequent variations of load due to working conditions affect the performance of the proposed hydraulic drive used in SDL machine. This section analyses the effects of the system parameter variations on the dynamics of the closed-circuit hydraulic drive system through model simulation. Such studies are essential for predicting the predictive behaviour of similar hydraulic drives from the application and design point of view. It is carried out by a small variation of

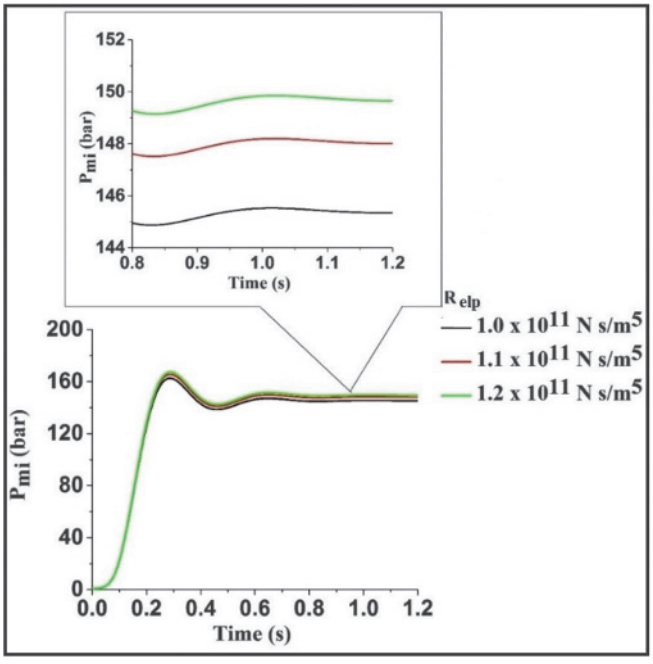

Fig.15: Effects of R_{elp} on the P_{mi}

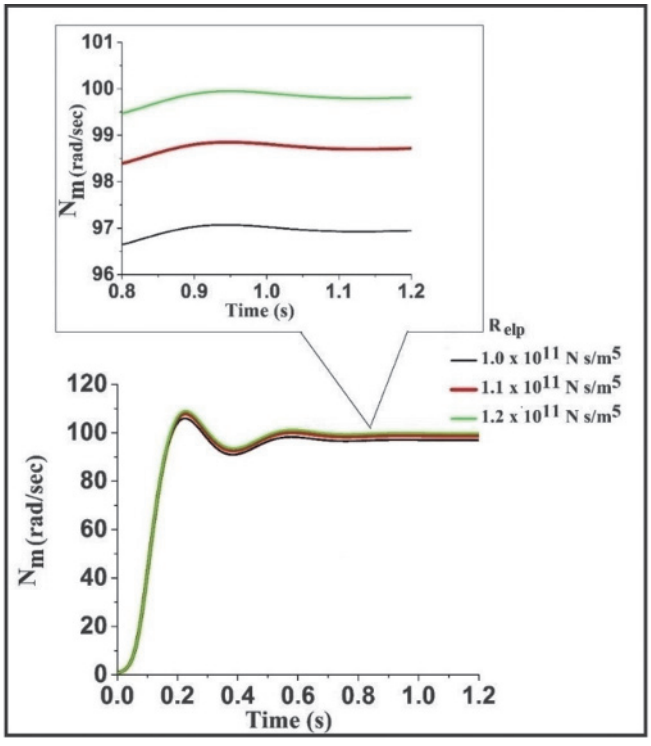

Fig.16: Effects of R_{elp} on the N_m

parameters by ±20% of its nominal values to verify the practical range of the hydrostatic drive's operation.

8.1 Influence of the pump leakage resistance (R_{ELP})

Figs.15 and 16 show the effects of R_{elp} on system pressure and speed. The R_{elp} of the pump decreases with the wear and tear of the hydrostatic components. It results in a decrease in the system pressure, drive speed, and motor torque. A decrease in the value of R_{elp} by 20% results in a drop in the hydro-motor speed of about 3 rad/s (≈3%). The settling time and peak rise time of the system responses remain almost unaffected. Similar responses would have obtained for R_{ilm}, R_{elm} of the hydro-motor.

8.2 Influence of the load torque (T_{LD}) on the hydraulic motor

Because of the varying ground condition and loading of the material by the SDL machine, the steady-state torque load (T_{ld}) on the hydrostatic drive changes. Figs.17 and 19 show the effects of variation of T_{ld} on the hydro-motor performance. The increase in T_{ld}, increases the system pressure and decreases the drive's speed. It results in less oscillatory system responses.

With the rise in T_{ld} from 2.25 Nm to 11.25 Nm, the peak rise pressure and the steady-state pressure increase by around 4% and 7%, respectively, and it also increases its peak rise time (230 ms to 235 ms). The nominal rise in the system pressure does not have much effect on the increase in the peak speed (3%) and the steady-state speed of the drive.

8.3 Influence of the effective bulk stiffness (K_B) of the fluid

The effective bulk stiffness K_b mainly depends on the bulk modulus of the fluid ($\hat{a}_o$) and also on the line length and flexibility of the hoses that depends on the drive system layout. Figures 19 and 20 indicate the dynamic behaviour of the P_{mi} and N_m. The rise in K_b leads to higher overshoot and more oscillatory system responses. In this case, the peak values of the pressure and speed increase 1500 rpm. Table 1 shows effect of system parameter variation on the simulation model response.

Table 1: Effect of system parameter variation on the simulation model response

Transient specification / Increasing paramete value	t_r	t_p	% of overshoot	t_s
R_{elp}	≈	▬	Δ	▬
T_{ld}	≈	Δ	∇	▬
K_b	∇	∇	Δ	Δ

ΔIncreasing; ∇Decreasing; ▬Unaffected; ≈Small change

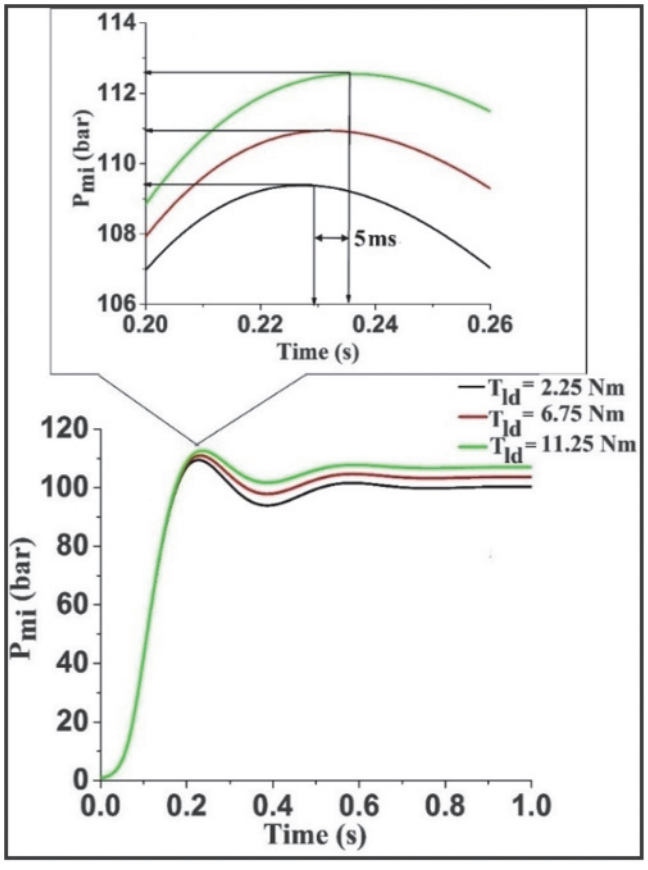

Fig.17: Effects of T_{ld} on the P_{mi}

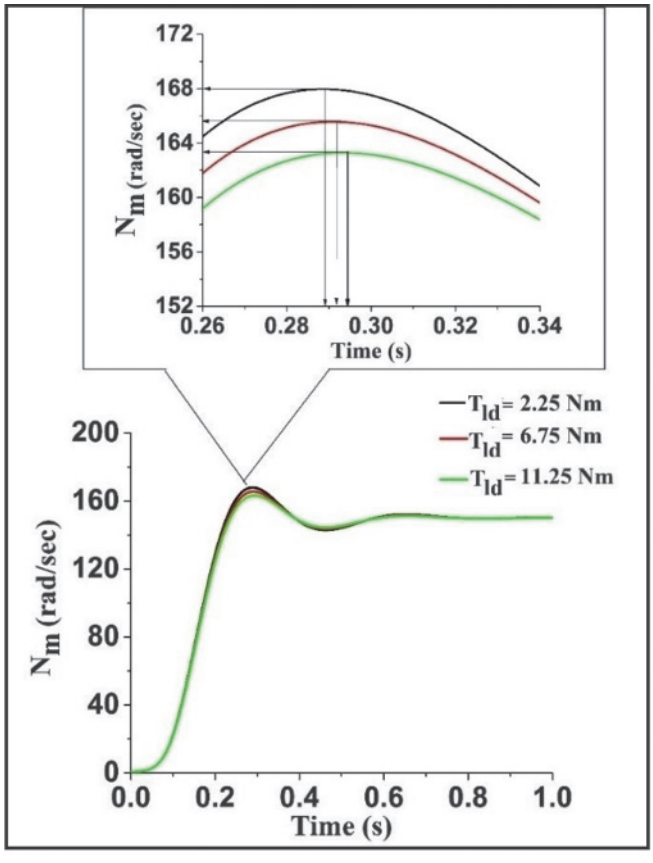

Fig.18: Effects of T_{ld} on the N_m

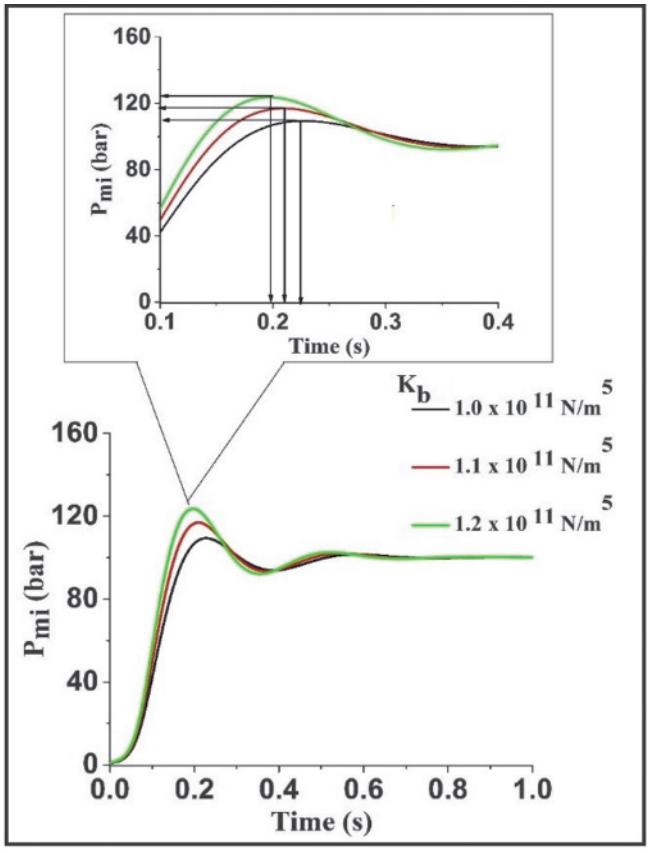

Fig.19: Effects of K_b on the P_{mi}

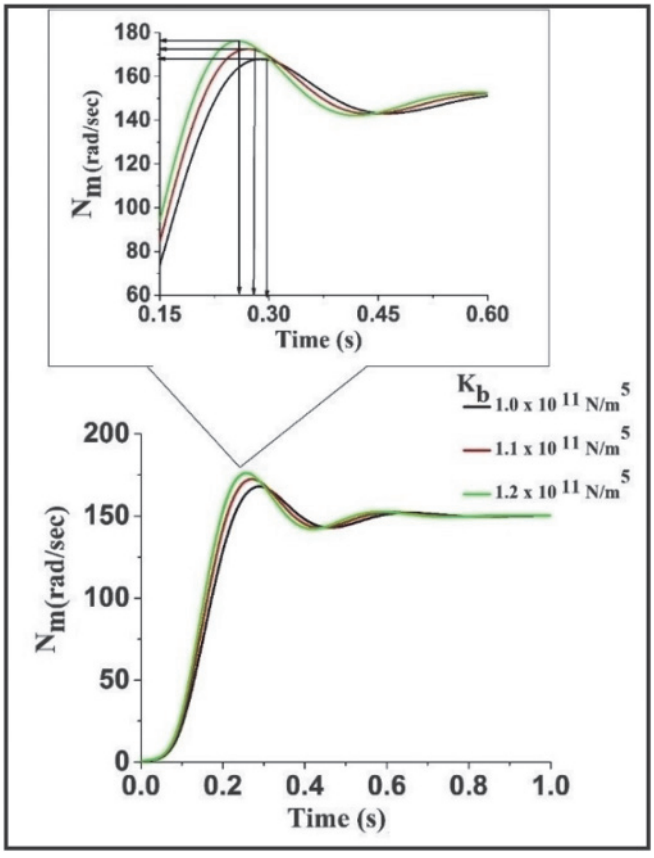

Fig.20: Effects of K_b on the N_m

Conclusions

The study conducted here represents the steady-state and sensitivity analysis of a hydrostatic transmission similar to that used in SDL. A multi-bondgpah representation of the hydrostatic drive system is made, from where a deduced model is developed which has been verified experimentally.

In the model various leakageflow and torque losses are taken in account for the resistive elements. Their relationship with the other system variables are retrieved from the reduced model and validated experimentally. They are found to have non-linear relationship with the torque and the displacement setting of the piston pump and the bent axis hydro-motor. Using them, the performance parameters of the drive for its complete speed range are verified experimentally and thus the model is validated.

The proposed method of creating efficiency for such machines may be useful to calculate the overall efficiency of a system in which they are applied. The sensitivity analysis of the system parameters has been studied over practical range of its variation to establish its feasibility.

Without using a special measurement technique and dismantling of the components, the system parameters are identified from the direct exploitation of the test data. The model fairly represents the behaviour of the plant, and therefore, it may be useful to the application engineers for the initial selection of similar hydraulic drive.

The proposed method of predicting the performance of the hydrostatic drive may be useful for selecting the identical machine for a given application. To optimize the drive efficiency, suitable and precise control scheme may be employed to vary the piston pump or the motor displacement setting or both which may be the scope of future work.

References

1. Rydberg. K. E., (2002): 'Concept and development trends for efficiency improvements of hydrostatics in mobile application, SAE Transaction, *Journal of commercial vehicles,* no. 1422, pp. 457-464.
2. Murrenhoff. H., (1999): 'Systematic approach to the control of hydraulic drives', Proc. Of Instn. Mech. Engrs., vol. 213, Part I, pp. 333-347.
3. Helduser. S., (1999): 'Electric-hydrostatic drive – an innovative energy-saving power and motion control system', I.MechE, Part-I, vol. 213, pp. 427-437.
4. Mandal S K, Dasgupta K, Pan S, and Chattopadhyay A. (2009): Theoretical and experimental studies on the steady-state performance of low-speed high-torque hydrostatic drives. Part 1: Modelling, Proc Inst Mech

Eng Part C, 223: 2663-2674.

5. Mandal S K, Dasgupta K, Pan S, and Chattopadhyay A. (2009): Theoretical and experimental studies on the steady-state performance of low-speed high-torque hydrostatic drives. Part 2: Experimental investigation, Proc Inst Mech Eng Part C, 223: 2675-2685.
6. Kumar. N., Dasgupta. K., (2009): 'Steady-state performance investigation of hydrostatic summation drive using bent-axis hydraulic motor', Proc Inst Mech Eng Part C.
7. Wang Y, Shengrong GU, Hongkang DO. (2018): Modelling and control of a novel electro-hydrostatic actuator with adaptive pump displacement. *Chinese Journal of Aeronautics*. 2018 Jun 21; https://doi.org/10.1016/j.cja. 2018.05.020.
8. Pfiffiner. R., Guzzdlla. L. and Onder. C. H., (2003): 'Fuel-optimal control of CVT power trains', Control Engg. Pract., 11(3), pp. 329-336.
9. Pettersson Karl and Tikkanen Seppo, (2004): 'Secondary control in construction machinery- design and evaluation of an excavator swing drive', The 11th Scandinavian International Conference on Fluid power: SICFP'09, June 2-4, Linkoping, Sweden.
10. Rahmfeld Robert, Skirde Eckhard, (2010): 'Efficiency measurement and mdelling – essential for optimising hydrostatic systems', 7th International fluid power conference, Aachen, pp. 1-14.
11. Manring Noah D., (2003): 'Mapping the efficiency for a hydrostatic transmission', *Journal of dynamic systems measurements and control*, Transaction of ASME, vol. 138, March, 2016, pp. 031004-1 – 031004-8.
12. Wang, Y., Zhang, Z. & Qin, Xq. (2014): Modelling and control for hydraulic transmission of unmanned ground vehicle. *J. Cent. South Univ.* 21, 124–129. https://doi.org/10.1007/s11771-014-1923-6
13. Tang, Hs., Yin, Yb., Zhang, Y. et al. (2016): Parametric analysis of thermal effect on hydrostatic slipper bearing capacity of axial piston pump. *J. Cent. South Univ.* 23, 333–343. https://doi.org/10.1007/s11771-016-3078-0
14. Fundamentals of fluid power controls , John Watton.
15. Product literature of the variable displacement bent axis hydro-motor, Bosch Rexroth (I) Ltd.
16. Product literature of the variable displacement in-line axial piston pump, Bosch Rexroth (I) Ltd.
17. McCandlish. D., Dorey. R. E., (1984): 'The mathematical modellin of the hydrostatic piston pumps and the motors', Proc. Instn of Mech. Engrs, 198 B(10), 165-174.
18. Thoma. J. U., (1969): 'Mathematical models and effective performance of hydrostatic machines and transmission', Hydraul. Pneumatic Power, 2, 642-651.
19. Schlosser. W. M. J., (1969): 'The overall efficiency of positive diaplacement piston pumps', *Hydl. Pneum. Power,* May, 272-280.